JCTC Journal of Chemical Theory and Computation

Article

pubs.acs.org/JCTC

Density of States Guided Møller–Plesset Perturbation Theory

Patrick J. Lestrange,[†] Bo Peng,[†] Feizhi Ding,[†] Gary W. Trucks,[‡] Michael J. Frisch,[‡] and Xiaosong Li*[,†]

[†]Department of Chemistry, University of Washington, Seattle, Washington 98195, United States

[‡]Gaussian, Inc. 340 Quinnipiac Street, Building 40, Wallingford, Connecticut 06492 United States

ABSTRACT: An integral formalism using a density-of-state framework has been developed for Møller–Plesset perturbation theory. This method is designed to compute the correlation energy correction for large systems with high density of states, such as polymers and nanostructures. The framework has the potential to lower the computational cost of perturbation theory, and such perspectives are discussed in this paper. This method has been implemented for the second- and third-order perturbation theory. Applications of the new methods to test cases of conjugated molecules show very good accuracy and significant savings in computational cost.

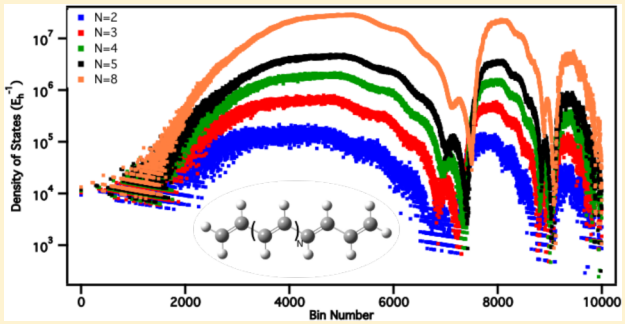

INTRODUCTION

An accurate description of many physical processes requires treatment of electron correlation beyond the mean-field approximation. Among various wave function based electronic structure theories, Møller–Plesset (MP) perturbation theory[1−3] is a relatively inexpensive and often reliable method of recovering most of the dynamic electron correlation. For example, the second-order formalism (MP2) improves the Hartree–Fock (HF) description of an electronic system by including a nonvariational electronic correlation energy correction, which can be computed as

$$E^{(2)} = -\sum_{\substack{i<j \\ a<b}} \frac{\langle ij||ab\rangle^2}{\epsilon_a + \epsilon_b - \epsilon_i - \epsilon_j} \tag{1}$$

where ϵ_i is a molecular orbital (MO) energy from the canonical HF orbitals. The two-electron repulsion integrals (ERIs) $\langle ij||ab\rangle = \langle ij|ab\rangle - \langle ij|ba\rangle$ are expressed in the MO basis. Following the common convention, the labels $i,j,...$ refer to the occupied MOs, the labels $a,b,...$ for the virtual MOs, and $p,q,...$ for generic MOs.

The ERIs in eq 1 are transformed from integrals in the atomic orbital (AO) basis,

$$\langle pq|rs\rangle = \sum_{\mu\nu\lambda\sigma} C^*_{\mu p} C^*_{\nu q} C_{\lambda r} C_{\sigma s} \langle \mu\nu|\lambda\sigma\rangle \tag{2}$$

where $\mu,\nu,...$ are indices for AOs, and the C's are MO coefficients. For large-scale systems, the disk requirement for storing ERIs can be circumvented by computing and transforming the necessary ERIs as needed using direct ab initio methodologies.[4−6] The ERI transformation from AO to MO basis scales as $O(N^5)$ with N being the total number of basis functions,[3,7] and is typically the bottleneck of the MP2 calculation.

The Laplace-transformed integral expression for the MP2 energy correction (LT-MP2) has been an area of interest for some time.[8,9] The elimination of the energy denominator in the expression has led to the development of a number of low-scaling MP2 algorithms for large-scale systems when effective integral screening approaches are used.[10−12] Recently, another technique that uses the complementary error function to eliminate the energy denominator has been developed for calculating the MP2 energy correction.[13] Both techniques have allowed for the study of much larger, periodic systems and their scaling can be improved by using a stochastic integration/sampling scheme.[13−15]

In this article, we propose another integral form of the MP energy expression that takes advantage of the high density of states (DOS) of certain systems. The subsequent sections will show that an algorithm guided by the DOS requires only a small fraction of the ERIs to be computed in order to achieve a reasonable approximation to the MP2 and MP3 energy corrections. Some computational details and benchmark tests are also described.

METHODOLOGY

Density-of-State Guided MP2. The derivation presented in this work starts with the well-known MP2 expression in the MO basis

$$E^{(2)} = -\sum_{\substack{i<j \\ a<b}} \frac{h_{ijab}}{\epsilon_{ijab}} \tag{3}$$

where $h_{ijab} = \langle ij||ab\rangle^2$ and $\epsilon_{ijab} = \epsilon_a + \epsilon_b - \epsilon_i - \epsilon_j$. When expressed as a function of the energy denominator, eq 3can be rewritten as

Received: August 29, 2013
Published: April 14, 2014

$$E^{(2)} = -\sum_k \frac{\overline{h}(\epsilon_k) n(\epsilon_k)}{\epsilon_k} \tag{4}$$

where the index k denotes the unique values of the energy denominator ϵ_k. The function $n(\epsilon_k)$ is the degeneracy at ϵ_k and $\overline{h}(\epsilon_k)$ is the average of the squared ERIs that correspond to the same ϵ_k.

For small molecules, the four-index energy denominator ϵ_k is a discrete spectrum as MO energies are mostly well-separated from each other. As a molecular system grows toward the bulk limit, the MO energies can often be described as continuous bands. At the bulk limit, the MP2 energy expression, eq 4, can be expressed as an integral over a continuous energy denominator

$$E^{(2)} = -\int_{\epsilon_{min}}^{\epsilon_{max}} \frac{\overline{h}(\epsilon)\rho(\epsilon)}{\epsilon} d\epsilon \tag{5}$$

The function $\rho(\epsilon)$ describes the density of states (DOS). A *state* in this context is defined as a unique two-electron substitution $(ij \rightarrow ab)$. Figure 1 shows the DOS distributions

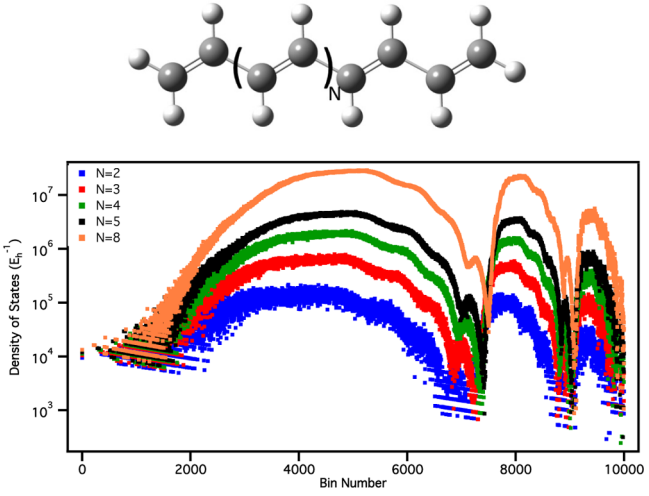

Figure 1. DOS for several polymer chains over 10 000 bins, DOS-MP2/6-31G(d). Blue, 4-carbon chain. Red, 6-carbon chain. Green, 8-carbon chain. Black, 10-carbon chain. Orange, 16-carbon chain. DOS is on a logarithmic scale for clarity.

for a series of conjugated polymers. As the size of the system increases, the DOS approaches a continuous function and the integral approximation becomes more reasonable.

For a semicontinuous ϵ spectrum, such as those exhibited in nanomaterials, eq 5 is best partitioned into a number of segments, M, with each segment defining separate sub-bands. These segments will be referred to as bins from now on.

$$E^{(2)} = -\sum_k^M \int_{\epsilon_k}^{\epsilon_k+\Delta\epsilon_k} \frac{\overline{h}_k(\epsilon)\rho_k(\epsilon)}{\epsilon} d\epsilon \tag{6}$$

It can be easily shown that eq 6 is equivalent to the conventional MP2 equation, eq 4 when $\Delta\epsilon_k \rightarrow 0$.

In practice, however, $\Delta\epsilon_k$ is chosen to be a realistically small energy range, and the ERI function $\overline{h}_k$ and the DOS function ρ_k need to be approximated. For semicondensed matters such as nanomaterials and short polymers, these functions can be approximated as constants with each bin. Our numerical tests presented in the following section suggest that these are good approximations for systems with band-like molecular orbital energy spectra as shown in Figure 1.

The first approximation was implemented by taking an average of the ERI function for the k-th bin

$$\overline{h}_k = \frac{1}{N_k} \sum_{\epsilon_{ijab} \in \epsilon_k} h_{ijab} \tag{7}$$

where N_k is the number of states in the k-th bin. The second approximation assumes a uniform distribution of states within the k-th bin and the DOS is treated as a constant

$$\overline{\rho}_k = \frac{N_k}{\Delta\epsilon_k} \tag{8}$$

With these two approximations, the MP2 energy can be computed as

$$E^{(2)} \approx -\sum_k^M \overline{h}_k \overline{\rho}_k \ln\left(\frac{\epsilon_k + \Delta\epsilon_k}{\epsilon_k}\right) \tag{9}$$

Equation 9 is our working equation to compute the MP2 energy correction in this paper. The computation of the MP2 energy correction is guided by the DOS function. A similar strategy has recently been used to calculate multiexciton generation rates in semiconductor nanocrystals.[16] In the following discussion, this method will be referred to as density of states guided MP2 (DOS-MP2).

DOS-MP3. This density-of-state guided technique can be generalized to any order in the Møller−Plesset perturbation series. For example, the MP3 energy expression is

$$E^{(3)} = \frac{1}{8}\sum_{ijabcd} \frac{\langle ij||ab\rangle\langle ab||cd\rangle\langle ij||cd\rangle}{\epsilon_{ijab}\epsilon_{ijcd}} + \frac{1}{8}\sum_{ijklab} \frac{\langle ij||ab\rangle\langle ij||kl\rangle\langle kl||ab\rangle}{\epsilon_{ijab}\epsilon_{klab}} + \sum_{ijkabc} \frac{\langle ij||ab\rangle\langle kb||cj\rangle\langle ac||ik\rangle}{\epsilon_{ijab}\epsilon_{ikac}}$$

Because each term has different summation bounds, they will all be evaluated independently. The first term will be used to illustrate the similarities between the second- and third-order DOS-MP3 expressions

$$E_1^{(3)} = \frac{1}{8}\sum_{ijabcd} \frac{g_{ijabcd}}{\lambda_{ijabcd}} \tag{10}$$

where $g_{ijabcd} = h_{ijab}h_{abcd}h_{ijcd}$ and $\lambda_{ijabcd} = \epsilon_{ijab}\epsilon_{ijcd}$.

The numerator g_{ijabcd} is a function of λ and the expression can be changed to a summation over its discrete values

$$E_1^{(3)} = \frac{1}{8}\sum_k \frac{\overline{g}(\lambda_k) n(\lambda_k)}{\lambda_k} \tag{11}$$

where $\overline{g}(\lambda_k)$ is the average of the ERIs corresponding to that value of λ_k and $n(\lambda_k)$ is the degeneracy at λ_k.

As with DOS-MP2, the above equation can be reformulated as an integration over the range of λ with the inclusion of a density, $\rho(\lambda)$. The integration can then be split into different segments over the range of λ

$$E_1^{(3)} = \frac{1}{8}\sum_k^M \int_{\lambda_k}^{\lambda_k+\Delta\lambda_k} \frac{\overline{g}_k(\lambda)\rho_k(\lambda)}{\lambda} d\lambda \tag{12}$$

dx.doi.org/10.1021/ct400765a | J. Chem. Theory Comput. 2014, 10, 1910−1914

With the assumption that $\overline{g}$ and ρ are constant over the range λ_k to $\lambda_k + \Delta\lambda_k$, the working equation is

$$E_1^{(3)} \approx \sum_k^M \overline{g}_k \overline{\rho}_k \ln\left(\frac{\lambda_k + \Delta\lambda_k}{\lambda_k}\right) \quad (13)$$

where $\overline{\rho}_k$ implicitly includes the prefactor 1/8. The other terms in the MP3 energy expression will have similar expressions, but with different definitions of $\overline{g}$ and λ.

The scheme used for the ERI averages in this implementation will be detailed in the following section. The accuracy and the computational savings of this technique will be discussed in the Results and Discussion section.

NUMERICAL IMPLEMENTATION

In this section, we present a detailed numerical implementation of eq 9 for the DOS-MP2 method. Because the DOS-MP3 working equation, eq 13, is basically the same as that for DOS-MP2, the implementation scheme presented herein can be generalized to DOS-MP3. We will only address the differences between DOS-MP2 and DOS-MP3 implementations whenever possible confusion could arise.

Binning MP Energy Denominator. Given a set of HF MO energies $\{\epsilon_p\}$, the limits of the MP energy denominator are determined using the lowest/highest unoccupied orbitals (LUMO/HUMO) and the lowest/highest occupied orbitals (LOMO/HOMO), $\epsilon_{min} = 2 \times (\epsilon_{LUMO} - \epsilon_{HOMO})$ and $\epsilon_{max} = 2 \times (\epsilon_{HUMO} - \epsilon_{LOMO})$. M number of bins are defined in $(\epsilon_{min}, \epsilon_{max})$ and the limit of each bin is $\epsilon_k \le \epsilon < \epsilon_{k+1}$ (note that the upper and lower bounds are ϵ_{min}^2 and ϵ_{max}^2 for DOS-MP3). Among various choices for binning the MP2 energy denominator ϵ into M segments, we use a logarithmic bin in this work, i.e., $\ln(\epsilon_k + \Delta\epsilon_k/\epsilon_k) = \Delta B$ = const where $\Delta\epsilon_k$ is the bin size. This technique naturally ensures that smaller bins are assigned over the range where the MP2 energy denominator ϵ is varying greatly and larger bins over the range where there is little variation. As a result, consistently better results were obtained with the logarithmic bins as opposed to bins of constant size.

Evaluating the Average ERI Functions. Evaluating the ERI function $\overline{h}_k$ is a crucial step that determines the accuracy and computational cost of the DOS-MPn method. We propose to sample only a certain fraction of the ERIs to obtain the average ERI function $\overline{h}_k$. To maintain the predictability of the method, we choose to use a fixed sampling frequency, e.g., one in every ten ERI products in the four-index loop, instead of a stochastic technique.[17,18] Even if a certain estimated ERI function, $\overline{h}_k/\overline{g}_k$, exhibits relatively large deviations from the true ERI function, $h_k(\epsilon)/g_k(\epsilon)$, its contribution to total error in the MP2/MP3 energy is only a fraction of the M number of bins. As the system size grows, the molecular orbital energy will approach a band-like spectra, reducing the error.

For a given sampled MPn term, there exists a simple expression, e.g., $k = [\ln \epsilon_{ijab} - \epsilon_{min}/\Delta B] + 1$ for DOS-MP2, to directly assign each state to the corresponding bin and add it to the number of states N_k in each bin. This is a very fast linear-scaling algorithm arising from the logarithmic binning scheme. After sampled terms are sorted into a particular bin, the density of states for the k-th bin is then calculated, $\overline{\rho}_k = \zeta N_k/\Delta\epsilon_k$, where $\zeta = N_{total}/\sum_k N_k$ accounts for the incomplete sampling space compared to the full space N_{total}.

RESULTS AND DISCUSSION

The DOS-MP2/MP3 algorithm presented herein is implemented by interfacing with the ERI evaluation routines in the development version of the Gaussian computational chemistry package.[19] 1000 bins are used for each DOS-MP2/MP3 calculation. For the test cases used in this work, increasing the number of bins used does not significantly change the computational accuracy.

The two test sets chosen in this work consist of conjugated polyacetylenes and polyacenes (Figure 2 left and right, respectively). The delocalized nature of the π bonds are the building blocks of continuous bands. Such systems represent prototypes for which the DOS-MPn method is designed. Table 1 lists the perturbation energy corrections for selected test molecules, comparing results obtained from conventional MPn and DOS-MPn methods. DOS-MPn corrections were obtained using 20% of ERIs to compute the average ERI functions. For smaller test molecules, such as 4-polyacetylene and 4-polyacene, DOS-MPn methods are able to obtain the majority of MPn corrections. As previously discussed, the DOS-MPn method is designed for large systems that exhibit a continuous energy spectrum. The percent error is expected to decrease as the system grows larger, and eventually converge to the exact result as the system approaches the bulk limit. For the 12-polyacene test molecule, DOS-MPn corrections, which use 20% of ERIs to estimate $\overline{h}_k$ in eq 9 and $\overline{g}_k$ in eq 13, exhibit only ~1% errors compared to conventional MPn results.

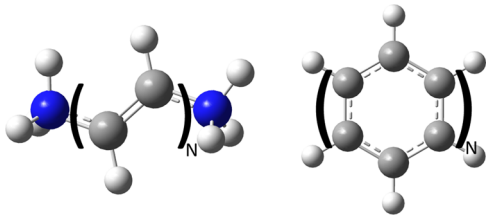

Figure 2. n-polyacetylene (left) and n-polyacene (right).

Figures 3 and 4 show the trend of percent errors of DOS-MPn as a function of the increasing polymer length for n-polyacetylenes and n-polyacenes, respectively. Three different sampling schemes (20%, 10% and 5%) are tested. As the number of molecular orbitals increases, the continuous band approximation in DOS-MPn becomes more reasonable for these types of systems. As a result, the percent error for DOS-MPn decreases quickly as the conjugation length increases and the molecular orbital energy spectrum becomes more band like. The same trend holds for all sampling schemes tested herein. The percent error of DOS-MPn is the smallest for the longest conjugated polymer tested here, even though the absolute MP2 and MP3 energy corrections are the largest. At the test set limit, the percent error is less than 0.5% for the 20% sampling case, and only ~2% for the 5% sampling case.

The advantage of the DOS-MPn method lies in its computational saving arising from using only a fraction of ERIs. The MP2 and MP3 methods formally scale as $O(N^4)$ and $O(N^6)$, respectively. The conventional ERI formation relies on an $O(N^5)$ transformation from AO to MO basis. As a result, the computational saving of the DOS-MP2 method will not reduce the leading cost in the perturbation theory. The advantage in terms of computational cost of the DOS-MPn method becomes apparent when $n \ge 3$. Figure 5 plots the relative computational

dx.doi.org/10.1021/ct400765a | J. Chem. Theory Comput. 2014, 10, 1910−1914

Table 1. MP2/STO-3G and MP3/STO-3G Energy Corrections for Selected Polyacetylenes and Polyacenes Expressed in E_h (a.u.)[a]

molecule	MP2	DOS-MP2	error%	MP3	DOS-MP3	error%
4-polyacetylene	−0.550 722	−0.465 259	15.5	−0.090 596	−0.065 166	28.1
8-polyacetylene	−1.012 753	−0.928 750	8.3	−0.159 628	−0.150 362	5.8
16-polyacetylene	−1.942 900	−1.876 146	3.4	−0.305 116	−0.304 762	0.1
4-polyacene	−1.038 196	−1.027 676	1.0	−0.126 984	−0.106 844	15.8
8-polyacene	−1.976 804	−2.003 664	1.4	−0.232 341	−0.229 656	1.2
12-polyacene	−2.917 785	−2.876 316	1.4	−0.338 058	−0.336 240	0.5

[a]Core orbitals are not included in the MP*n* energy correction evaluations. $E_{\mathrm{DOS-MPn}}$ and E_{MPn} are the energy corrections computed using the DOS-MP*n* and conventional MP*n* methods. DOS-MP*n* corrections were obtained using only 20% of ERIs. Error% is computed as $((|E_{\mathrm{DOS-MP}n} - E_{\mathrm{MP}n}|)/E_{\mathrm{MP}n})\%$.

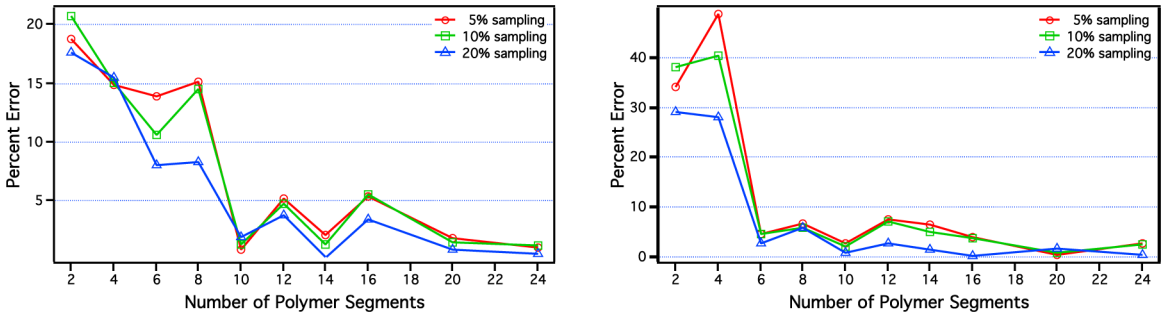

Figure 3. Percent error as a function of the *n*-polyacetylenes polymer length computed at the DOS-MP*n*/STO-3G level of theory (left, DOS-MP2; right, DOS-MP3). Results using different sampling schemes are compared with the conventional MP*n* methods. Error% is computed as $((|E_{\mathrm{DOS-MP}n} - E_{\mathrm{MP}n}|)/E_{\mathrm{MP}n})\%$.

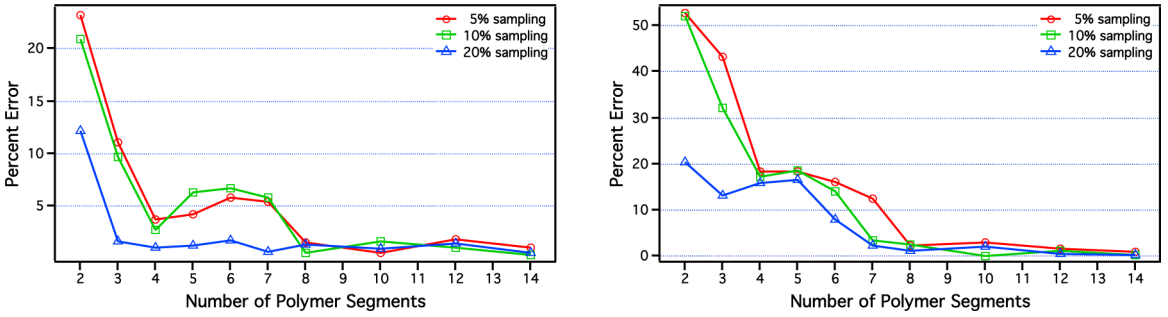

Figure 4. Percent error as a function of the *n*-polyacenes polymer length computed at the DOS-MP*n*/STO-3G level of theory (left, DOS-MP2; right, DOS-MP3). Results using different sampling schemes are compared with the conventional MP*n* methods. Error% is computed as $((|E_{\mathrm{DOS-MP}n} - E_{\mathrm{MP}n}|)/E_{\mathrm{MP}n})\%$.

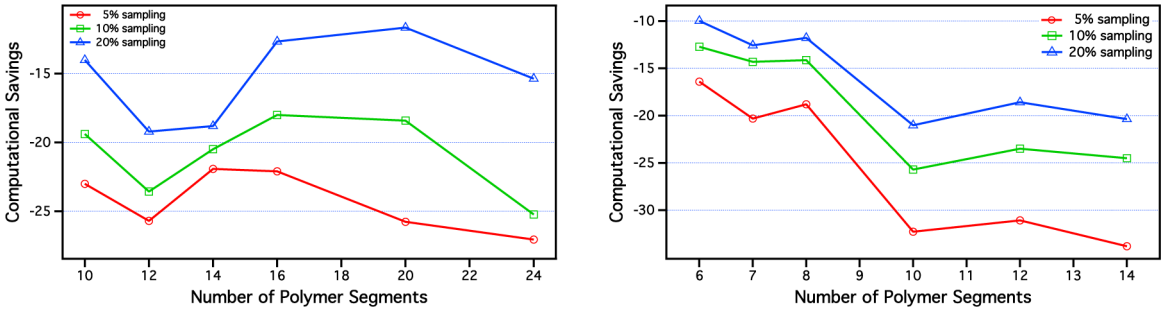

Figure 5. Relative computational cost of the DOS-MP3 method (left, *n*-polyacetylenes; right, *n*-polyacenes). The relative computational cost is computed using $((T_{\mathrm{DOS-MP3}} - T_{\mathrm{MP3}})/T_{\mathrm{MP3}})\%$ where $T_{\mathrm{DOS-MP3}}$ and T_{MP3} are the CPU times of DOS-MP3 and conventional MP3 methods. Computational costs for small test cases are not plotted because the absolute CPU times are small so that the uncertainty is large.

costs for the DOS-MP3 method with various sampling rates compared to the conventional approach. The computational saving increases as the sampling rate decreases as expected from the formalism of the DOS-MP*n* method. For the 5% sampling case, DOS-MP3 method exhibits a 20%−30% saving in computational cost for larger test cases, while the percent error is still within 2% at the test set limit. Optimization of the DOS-MP*n* code could further reduce the computational cost.

dx.doi.org/10.1021/ct400765a | J. Chem. Theory Comput. 2014, 10, 1910−1914

CONCLUSION

We have proposed a new integral expression and algorithm for the evaluation of the MP*n* energy correction guided by a density-of-state technique. This algorithm uses only a small portion of the ERIs to evaluate the MP*n* energy while maintaining very good accuracy. The high accuracy arises from binning the ERIs according to their corresponding MO energy spectrum. Even if the estimated ERI function exhibits relatively large deviations from the true ERI function, its contribution to total error in the MP*n* energy is only a fraction of the M number of bins. On the other hand, as the method is designed to address a semicontinuous MP*n* energy spectrum, one would expect increased accuracy and stability (smaller standard deviation) as the system size grows. Because only a small fraction of the ERIs are used in computing the MP*n* corrections, there is an advantage of using the DOS-MP*n* method to reduce the computational cost of perturbation theory. Computational tests on conjugated polyacetylenes and polyacenes of increasing chain lengths show significant computational savings with a reasonable accuracy.

AUTHOR INFORMATION

Corresponding Author

*X. Li. E-mail: li@chem.washington.edu.

Notes

The authors declare no competing financial interest.

ACKNOWLEDGMENTS

Financial support from the US National Science Foundation (Grant Nos. CHE-0844999 and CHE-1265945 to X.L.), and additional support from Gaussian, Inc. and the University of Washington Student Technology and Royalty Research Fund are gratefully acknowledged.

REFERENCES

(1) Møller, C.; Plesset, M. S. *Phys. Rev.* **1934**, *46*, 618−622.
(2) Bartlett, R. J. *Annu. Rev. Phys. Chem.* **1981**, *32*, 359−401.
(3) Szabo, A.; Ostlund, N. S. *Modern Quantum Chemistry: Introduction to Advanced Electronic Structure Theory*; Dover Publications: Mineola, NY, 1996.
(4) Sæbø, S.; Almlöf, J. *Chem. Phys. Lett.* **1989**, *154*, 83−89.
(5) Head-Gordon, M.; Pople, J. A.; Frisch, M. J. *Chem. Phys. Lett.* **1988**, *153*, 503−506.
(6) Frisch, M. J.; Head-Gordon, M.; Pople, J. A. *Chem. Phys. Lett.* **1990**, *166*, 281−289.
(7) Schlegel, H. B.; Frisch, M. J.. In *Theoretical and Computational Models for Organic Chemistry*; Formosinho, S. J.; Csizmadia, I. G.; Arnaut, L. G., Eds.; Springer: Dordrecht, The Netherlands, 1991; pp 5−33.
(8) Almlöf, J. *Chem. Phys. Lett.* **1991**, *181*, 319−320.
(9) Häser, M.; Almlöf, J. *J. Chem. Phys.* **1992**, *96*, 489−494.
(10) Ayala, P. Y.; Scuseria, G. E. *J. Chem. Phys.* **1999**, *110*, 3660−3671.
(11) Doser, B.; Lambrecht, D. S.; Kussmann, J.; Ochsenfeld, C. *J. Chem. Phys.* **2009**, *130*, 064107.
(12) Maurer, S. A.; Lambrecht, D. S.; Kussmann, J.; Ochsenfeld, C. *J. Chem. Phys.* **2013**, *138*, 014101.
(13) Neuhauser, D.; Rabani, E.; Baer, R. *J. Chem. Theory Comput.* **2013**, *9*, 24−27.
(14) Ayala, P. Y.; Kudin, K. N.; Scuseria, G. E. *J. Chem. Phys.* **2001**, *115*, 9698−9707.
(15) Willow, S. Y.; Kim, K. S.; Hirata, S. *J. Chem. Phys.* **2012**, *137*, 204122.
(16) Baer, R.; Rabani, E. *Nano Lett.* **2012**, *12*, 2123−2128.
(17) Neuhauser, D.; Rabani, E.; Baer, R. *J. Phys. Chem. Lett.* **2013**, *4*, 1172−1176.
(18) Baer, R.; Neuhauser, D.; Rabani, E. *Phys. Rev. Lett.* **2013**, *111*, 106402.
(19) Frisch, M. J.; Trucks, G. W.; Schlegel, H. B.; Scuseria, G. E.; Robb, M. A.; Cheeseman, J. R.; Scalmani, G.; Barone, V.; Mennucci, B.; Petersson, G. A.; Nakatsuji, H.; Caricato, M.; Li, X.; Hratchian, H. P.; Izmaylov, A. F.; Bloino, J.; Zheng, G.; Sonnenberg, J. L.; Liang, W.; Hada, M.; Ehara, M.; Toyota, K.; Fukuda, R.; Hasegawa, J.; Ishida, M.; Nakajima, T.; Honda, Y.; Kitao, O.; Nakai, H.; Vreven, T.; J, A. Montgomery, J.; Peralta, J. E.; Ogliaro, F.; Bearpark, M.; Heyd, J. J.; Brothers, E.; Kudin, K. N.; Staroverov, V. N.; Keith, T.; Kobayashi, R.; Normand, J.; Raghavachari, K.; Rendell, A.; Burant, J. C.; Iyengar, S. S.; Tomasi, J.; Cossi, M.; Rega, N.; Millam, J. M.; Klene, M.; Knox, J. E.; Cross, J. B.; Bakken, V.; Adamo, C.; Jaramillo, J.; Gomperts, R.; Stratmann, R. E.; Yazyev, O.; Austin, A. J.; Cammi, R.; Pomelli, C.; Ochterski, J. W.; Martin, R. L.; Morokuma, K.; Zakrzewski, V. G.; Voth, G. A.; Salvador, P.; Dannenberg, J. J.; Dapprich, S.; Parandekar, P. V.; Mayhall, N. J.; Daniels, A. D.; Farkas, O.; Foresman, J. B.; Ortiz, J. V.; Cioslowski, J.; Fox, D. J. *Gaussian Development Version*, Revision H.28. Gaussian Inc.: Wallingford CT, 2012.